ASIA-PACIFIC SOLAR RESEARCH CONFERENCE
Peer Reviewed
2016 Solar Research Conference
2016

Yuan-chih,Chang

Nanosphere Lithography for Fast and Controlled Fabrication of Large Area Plasmonic Nanostructures in Thin Film Photovoltaics

Yuanchih Chang, Michael E. Pollard, David N. R. Payne,
Supriya Pillai, and Darren M. Bagnall

School of Photovoltaic and Renewable Energy Engineering,

University of New South Wales, Sydney, NSW 2052, AUSTRALIA

E-mail: y.chang@student.unsw.edu.au

Abstract

Plasmonic nanostructure arrays have demonstrated potential for enhanced light trapping in thin-film solar cells. However, the fabrication processes often used, such as e-beam lithography (EBL), are accompanied by high costs and low throughput, which prevent commercial use. Nanosphere lithography (NSL) has long been recognized as a promising alternative for physical masking, but achieving monolayer or bilayer colloidal films with high uniformity generally requires time-consuming deposition methods (e.g. Langmuir-Blodgett coating, convective self-assembly etc.). Here, we present an improved spin-coating deposition method for fast fabrication of large area plasmonic nanostructures in thin photovoltaic devices, which are critically reliant on effective light-trapping. Key spin-coating parameters such as spin speed, acceleration, and nanosphere (NS) concentration were systematically studied for polystyrene (PS) NS with diameters between 0.2µm and 0.99µm. The results show that the concentration of the PSNS solution has a greater influence than the spin speed and acceleration. For all PSNS sizes, the monolayer coverage and defect-free area can be greatly improved through adjustment of the PSNS concentration alone. Using this technique, high quality hexagonal monolayer NS masks can be quickly formed on any hydrophilic surface. The final array period and feature size can be easily modified by altering the size of the PSNS used and the parameters of the subsequent oxygen plasma etch process. Two types of large area (20mm×20mm) plasmonic nanostructures were fabricated using these uniform PSNS monolayers in order to demonstrate the feasibility of the spin-coated NSL technique for applications in c-Si photovoltaic devices. This work provides guidance for the efficient and controllable deposition of monolayer colloidal films, thereby allowing for the cost-effective fabrication of large scale plasmonic nanostructures for solar cell applications.

1. Introduction

The optical properties of plasmonic nanoparticle arrays have been heavily studied over the last decade[1], [2]. These arrays offer the potential for enhanced light trapping in photovoltaic cells thereby allowing significantly thinner devices and lower material cost [3]. However, the commercial adoption of such arrays has been limited due to the necessity of complicated and expensive fabrication process such as e-beam lithography (EBL). Although nanosphere

lithography (NSL) has long been recognized as a promising alternative, achieving monolayer or bilayer colloidal films with high uniformity generally requires time-consuming deposition methods (e.g. Langmuir-Blodgett coating, convective self-assembly etc.) [4]. These techniques have therefore remained unsuitable for high-throughput commercial production lines. Moreover, with improved growth methods pushing ultra-thin c-Si layers towards commercial viability, there is a growing need to develop economic processes for fast fabrication of large area plasmonic nanostructures. The higher quality c-Si material promises efficiencies much greater than typical amorphous silicon and microcrystalline silicon-based thin film solar cells.

The spin coating of NS suspensions onto a substrate accelerates the evaporation of the solvent, enabling monolayer or bilayer colloidal films to be rapidly formed [5], [6]. It therefore has higher potential for mass production in wafer-scale processes. The uniformity of the NS arrays is greatly affected by the spin speed, acceleration, the size of the nanospheres, the concentration of the NS suspension, and the wettability of the substrate surface. Silica and polystyrene NS are two of the more commonly used materials. Previous reports in the literature on spin coated NS arrays provide only limited data on the areal uniformity of the monolayers formed for a given NS size. Colson et al. used statistical experiment designs for exploring the significant degree of each spinning parameter in a three step spinning process [7]. They concluded that for achieving large-area close packed hexagonal NS arrays, a fast ramp up to a high rotation speed is required. This critical factor is based on adopting solvents having evaporation rates similar to water.-- Conversely, Choi et al. found that by using the organic solvent N,N-dimethyl-formamide (DMF), large-are closed pack hexagonal silica NS arrays could be achieved using a single step spinning process with a relatively slow acceleration rate [8]. However, the toxicity of DMF makes it less favourable than solvents such as de-ionized (DI) water or ethanol. Chen et al. reported a more detailed study on the spinning parameters for different size PSNS, using a mixture of ethanol and DI water (1:1, v/v) as the solvent. Their results corroborated the conclusions of Colson et al. [9]. However, the range of concentrations used in the experiment was relatively coarse, from 5% to 25%. Under certain spin conditions, the concentration of the suspensions used is known to strongly affect the uniformity of the deposited NS array [8][10]. It is therefore difficult to achieve highly repeatable results when using unknown NS solution concentrations, even under optimized coating conditions.

In this paper, we present an improved spin-coating deposition method for fast fabrication of large area plasmonic nanostructures in thin photovoltaic devices. Key spin-coating parameters such as spin speed, acceleration, and nanosphere (NS) concentration have been systematically studied for polystyrene (PS) NS with diameters from 0.2μm to 1μm. Processing and analysis of optical and electron microscope images was firstly used to evaluate the degree of uniformity and monolayer coverage of PS colloidal-crystal films. Through adjustment of the aforementioned parameters, high quality monolayer hexagonal NS masks could be formed within three minutes. With additional dry etch and lift-off processes, we were able to fabricate large scale plasmonic nanostructures and incorporate them into preliminary, proof-of-concept optical device stacks in order to demonstrate their potential for light trapping in thin silicon solar cells.

2. Experiment

2.1. Material and instrumentation

Polystyrene nanosphere suspensions with mean diameters of 0.2µm, 0.5µm, 0.76µm, and 0.99µm were prepared in-house. A mixture of ethanol and DI water (1:1,v/v) was used as the solvent. Each PSNS suspension was twice run through a centrifugal purification process, followed by 6 hours of ultrasonic agitation to ensure a uniform dispersion. The 20mm x 20mm silicon substrates were cleaned via sequential sonication in acetone and IPA. A hydrophilic silicon surface was achieved using ultraviolet (UV)/ozone treatment for 20 minutes.

In order to rapidly and fairly compare the uniformity of the deposited NS array, an automated image analysis function was written in MATLAB. This analysis was based on Fourier transformation of the optical and SEM images and subsequent integration of the Fourier spectrum across all angles. The uniformity of the NS arrays could then be established from the magnitude and FWHM of the Fourier components associated with diffraction from the NS arrays. Further details are provided in section 3.

Normal incidence optical absorption was used to characterize the subsequent absorption enhancement in the c-Si optical devices incorporating the NSL-fabricated plasmonic nanostructures.

2.2. Single-step spin-coating process

The single step spin coating process can be divided into four stages.

1. Firstly, ~50µL PS nanosphere suspension is pipetted onto the middle of the substrate and allowed to spread out statically.
2. Upon initiating the spinning, the increasing centrifugal force quickly pushes residual suspension away from the edge and the NS suspension starts to evaporate.
3. As the dropped suspension in the center of the substrate evaporates faster, the thinner liquid thickness raises the capillary force, which drives more NS from the edge toward the nucleus. The NS begin to assemble on the surface when the thickness of the liquid becomes smaller less than the diameter of the NS.
4. Finally, after complete solvent evaporation, monolayer/multilayer colloidal films are formed.

In our experiments, parameters such as spin speed, acceleration, and nanosphere (NS) concentration for 4 different size PSNS were systematically analyzed. For each PSNS size, a concentration of 10wt% was initially used as a baseline for exploring the protocols to allow large area monolayer films to form. The NS concentration was then adjusted to either a more diluted or a more concentrated value and tests run using the optimal spinning conditions obtained from the 10wt% baseline. Finally, the best spinning conditions were determined for the optimal concentrated NS suspensions.

2.3. Optical device fabrication flow

Two plasmonic nanostructures - Ag nanodisc arrays, and NS embedded arrays - are presented in this paper in order to demonstrate the feasibility of the cost-effective NSL fabrication

process. The process flow for each type of nanostructure is presented in Figure 1 and 2. The uniform NS arrays generated from the optimized spin-coating process acts either as a physical mask or can be used for directly providing plasmonic scattering in the device.

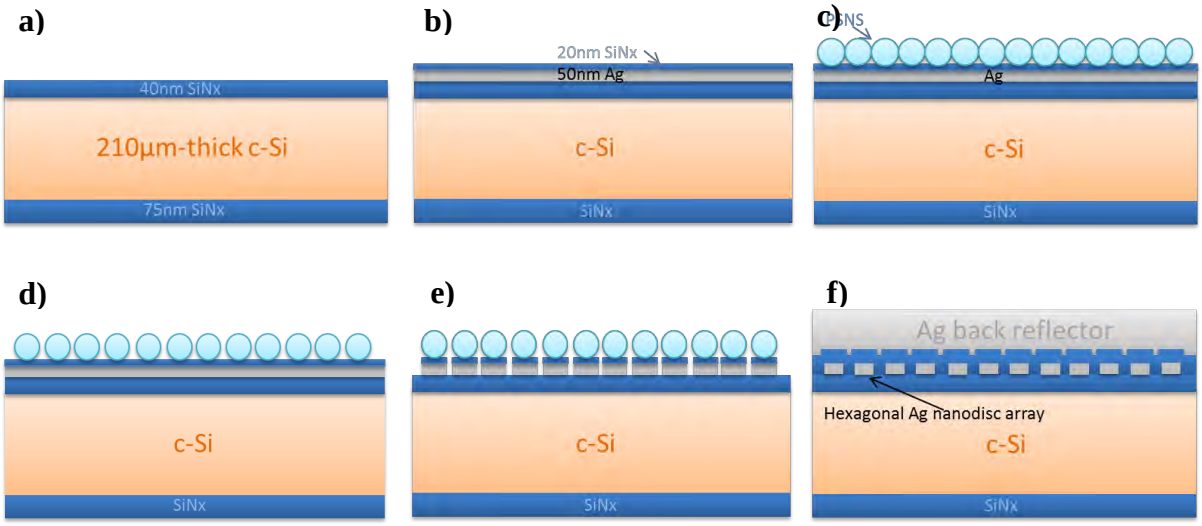

Figure 1 a-f Ag nanodisc arrays structure fabrication flow

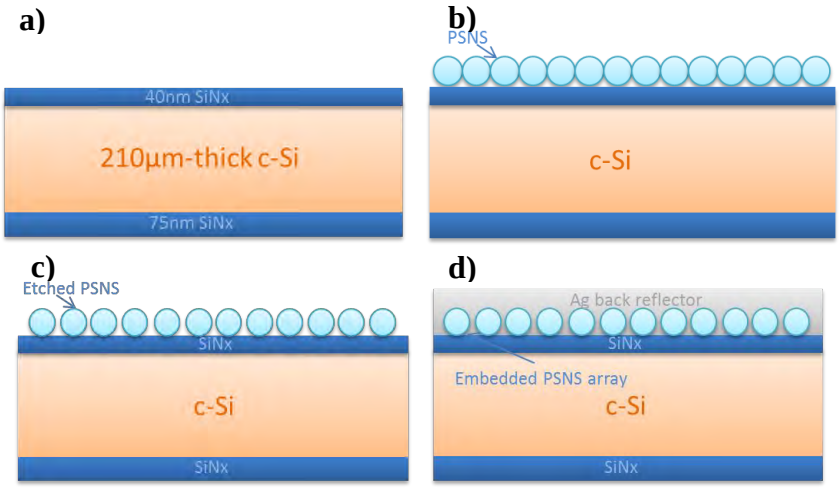

Figure 2 a-d NS embedded grating structure fabrication flow

A 75nm thick PECVD SiNx passivation layer was first deposited on the front of the silicon substrate, followed by a 40nm thick SiNx passivation layer on the rear (Figure 1a and 2a). For the Ag nanodisc arrays structure, a 50nm Ag layer was e-beam evaporated on the rear and subsequently coated with a 20nm thick layer of sputtered SiNx (Figure 1b). After spinning on the NS, (Figure 1c and Figure 2b), an oxygen plasma etch was used to reduce the diameter of the NS to an optimal size which was expected to yield the best absorption in simulation models with a semi-infinite c-Si absorber(Figure 1d and Figure 2c). For the Ag nanodisc arrays, Ar ion sputtering was used to transfer the NS mask into the SiNx and Ag layers (Figure 1e). The NS were removed by sonication in toluene and a 100nm layer of SiNx sputtered over the Ag nanodiscs. Finally, a ~1µm Ag back-contact was evaporated on both optical device samples (Figure 1f and 2d).

3. Results and discussion

3.1. Analyzing the uniformity of the deposited NS films

Quantitative comparison of the uniformity of the deposited NS films requires more than simple inspection of optical or SEM images. Low magnification optical images may not be able to clearly resolve grain boundaries and array orientation, while high magnification SEM images may provide misleading results owing to the small area examined. Although comparing a large number of SEM images under the same magnification can work, an automated analytical method is still desirable to minimize the unreliability due to operator bias and numerically quantify the array quality.

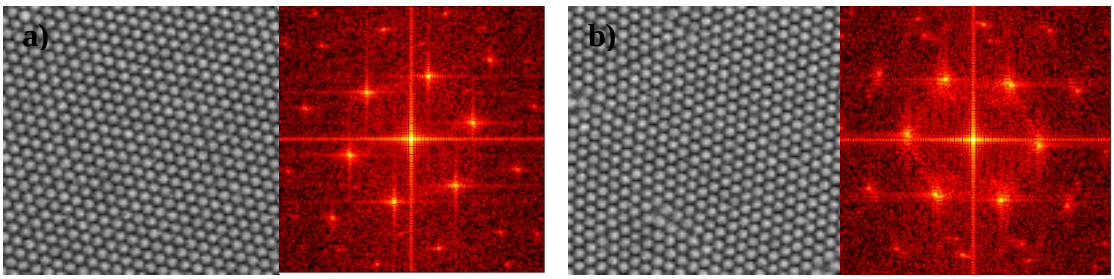

Figure 3 a) and b) Uniform closed pack hexagonal arrays with different orientations. Spatial domain SEM figure (left) and frequency domain profile (right)

Fourier transforms transfer the input SEM images from the spatial domain into the frequency domain. When a uniform close-packed hexagonal array is present in the input image, regular hexagonal patterns are clearly visible at spatial frequencies corresponding to the periodicity of the array and reflecting the symmetry of the lattice. The pattern orientation follows the orientation of the NS array (Figure 3). In low magnification (large area) SEM images, we typically observe 'grains' of close-packed NS with varying orientations, even though the whole surface may be covered by a monolayer array. The accumulation of individual hexagonal patterns with different rotations results in the frequency profile showing ring patterns. The appearance of a clear and sharp ring, with a spatial frequency matching the expected periodicity, indicates that the surface is covered by a uniform NS monolayer while the existence of defects (voids, clusters) makes this ring less distinguishable (Figure 4 and 5). By integrating the line profiles taken from the center to the edge over all in-plane angles, the quality of the NS films (Q) can be determined by both the relative intensities of the peak at the expected spatial frequency (h) and the background level, and the width of this peak.(W)

$$Q \equiv \sum_i \frac{h_i}{W_i}$$

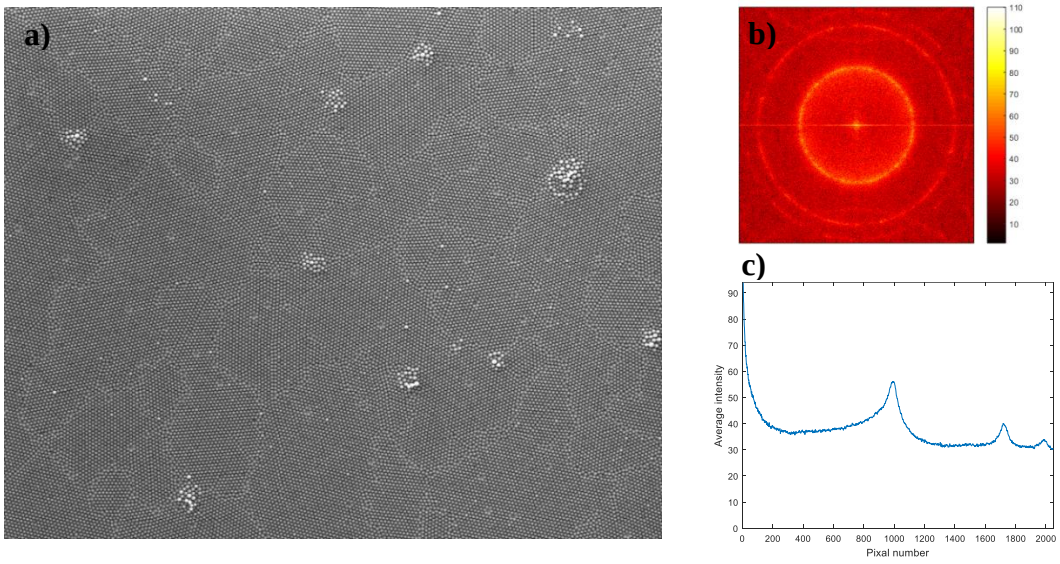

Figure 4 a) Spatial domain SEM image and b) frequency domain profile of a NS film with most area covered by uniform NS monolayers. c) Intensity line profile of the frequency domain profile integrated over all angles. The 0 point of the x-axis corresponds to the center point in b)

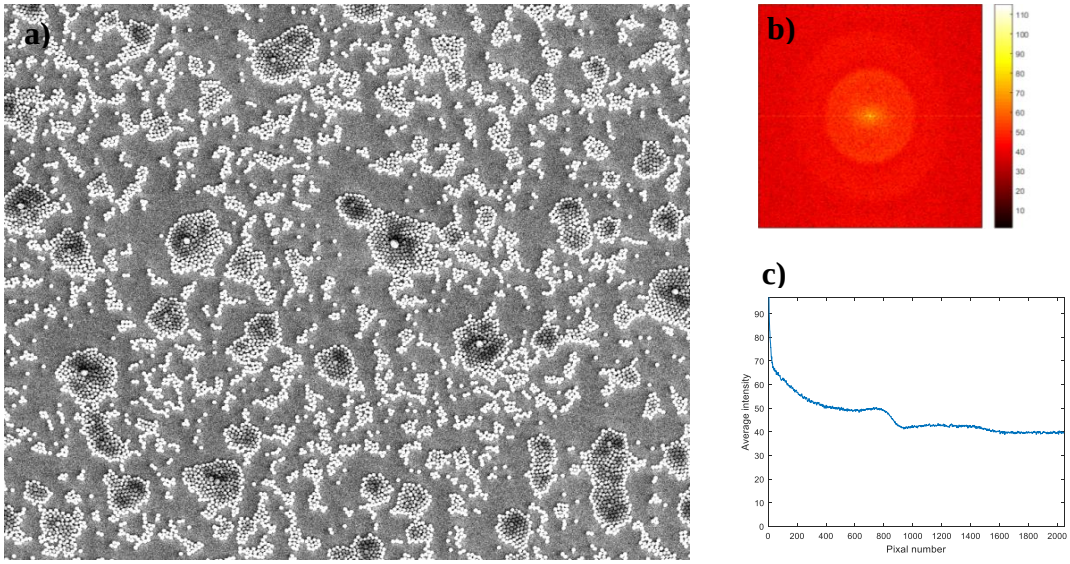

Figure 5 a) Spatial domain SEM image and b) frequency domain profile of a NS film with many defects and NS clusters. c) Intensity line profile of the frequency domain profile integrated over all angles. The 0 point of the x-axis corresponds to the center point in b)

3.2. The initial exploration of the spin conditions

In previous works, using the same spin speed and acceleration, it was generally found that higher concentration NS suspensions lead to more bilayer/multilayer areas while lower concentration NS suspensions leave larger voids in the monolayer film [8], [10], [11]. The optimal spinning conditions for forming monolayer films therefore clearly depend on the suspension concentration. In this work, we initially used different spinning conditions with a

fixed concentration (10wt%) for suspensions of each of the four NS diameters to examine the protocols for forming large area monolayer NS films.

In general, a low spin speed/acceleration lowers the uniformity of the deposited film and result in a higher incidence of bilayer/multilayer and NS islands. This is because a low spin speed/acceleration enhances the convective instability during the NS assembly step [11]. However, an extremely high spin speed or directly ramping up to the final spin speed (high acceleration) tends to leave large voids in the coating.

For NS diameters of 0.5µm, 0.76µm, and 0.99µm, the largest area of monolayer coverage was achieved by using a spin speed (1800rpm) with an 800 rpm/s ramp up. Moreover, quite a few bilayer regions were found in 0.5um size NS films and large areas free of particles were found between 0.99um size NS monolayer films. Firstly, a quick ramp up to the final spin speed enables just enough NS suspensions remain on the substrate before major solvents starting evaporating. Secondly, the spin speed affects the centrifuge force applied on the NS during the assembly step. This spin speed initially allows the interparticle distance of the center NS suitable for single layer capillary assembly. Then it offers a good balance between the shear force applied on the particles remaining in the NS suspension toward to the edge of the substrate and the evaporation rate of the solvent, which affects the viscosity of NS suspension. The well-built convective particle flux keeps bringing NS toward the capillary assembled region for forming long-range monolayer films. A high spin speed has a tendency to cast too much of the NS suspension off the substrate. The NS themselves also receive more net force towards the edge during the critical assembly stage, thus the monolayers formed exist in sparse and disordered domains. In contrast, a lower spin speed leaves too much NS suspension on the surface and thus more bilayer/multilayers are found. However, for the smallest size (0.2µm), the surface was predominantly covered by bilayer/multilayers regardless of the spinning conditions.

While the 0.2µm NS did not have a clearly optimal set of spin conditions, all three of the remaining NS sizes appeared to have the same optimal parameters. In addition, if the concentration of NS suspension only affects the monolayer coverage rate, it is expected that an increase/decrease of the NS suspension concentrations should lead to a better deposition result. Consequently, a medium spin speed (1800rpm) and a high acceleration (800rpm/s) were selected for further optimizing the concentration of NS suspensions.

3.3. Optimizing the NS suspension concentration

In the previous section, more bilayer/multilayers were found in small size NS films and larger voids were found in large size NS films. Depending on the NS size, suspension concentrations were therefore made either more dilute or more condensed to determine the optimal concentration. The optimal concentrations for maximizing the monolayer coverage, without introducing bilayer/multilayers, are shown in Figure 6 for each NS size. It is evident that the optimal concentration is approximately linearly proportional to the size of the PSNS.

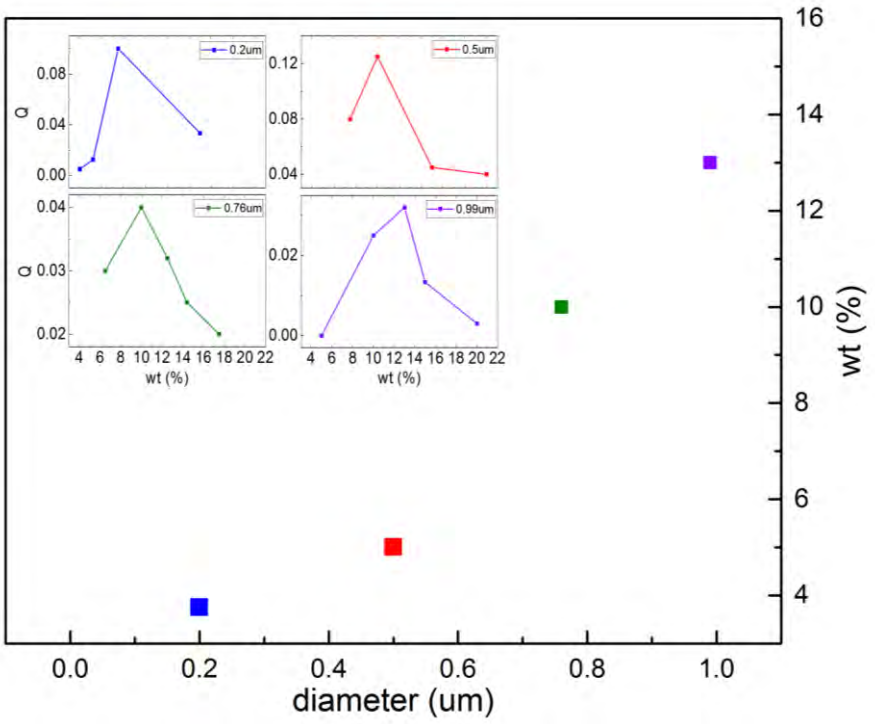

Figure 6 The optimal concentration of different size PSNS for forming large area uniform NS monolayers. (deposited by 1800rpm spin speed w/ 800rpm/s acceleration)

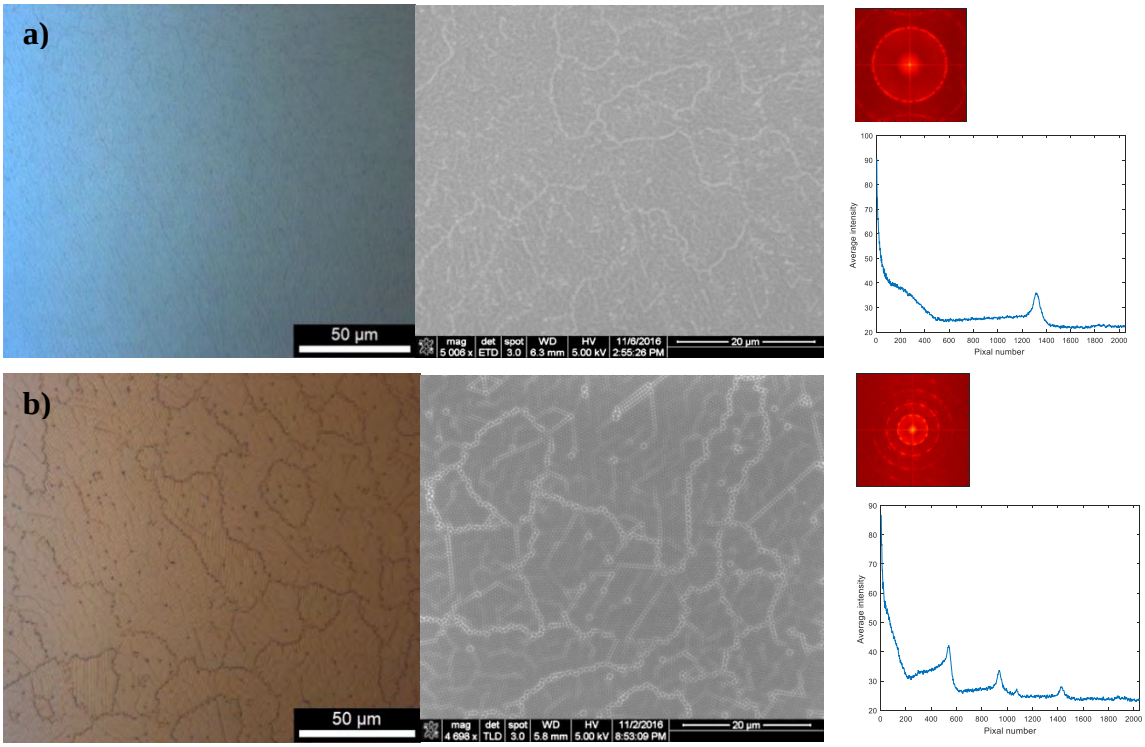

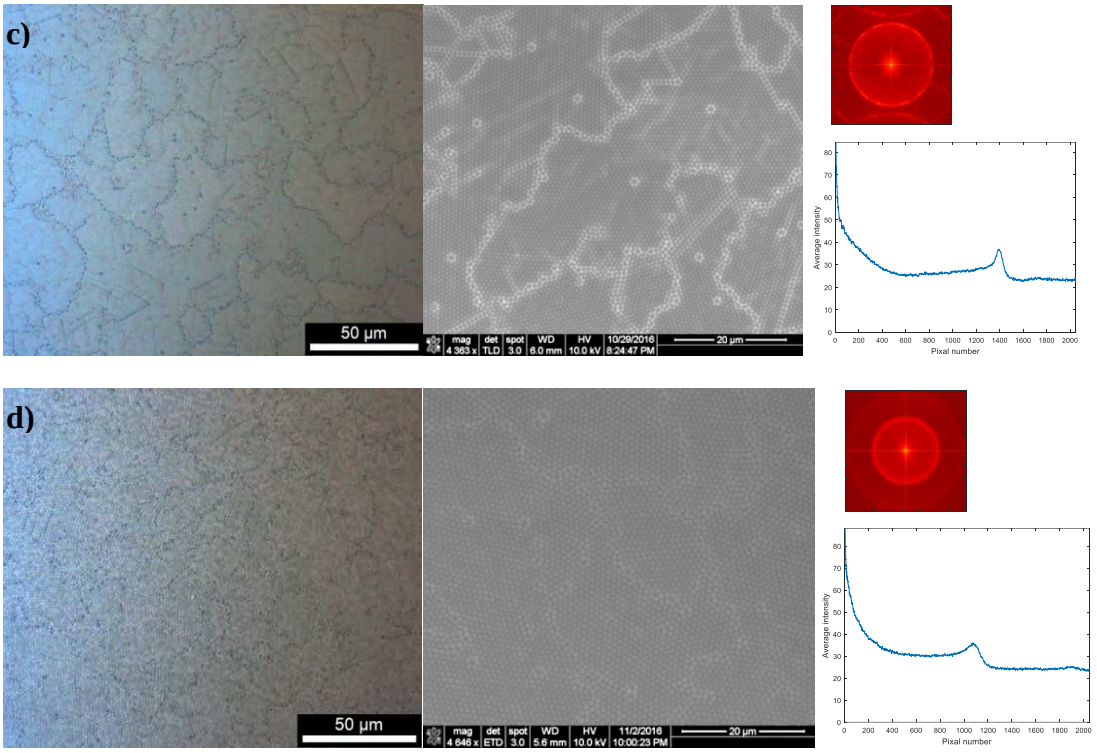

Figure 7 Large area uniform a)0.2µm b)0.5µm c) 0.76µm and d) 0.99µm monolayers deposited by NS suspensions with optimal concentrations. Each figure shows 100x magnification optical microscope, SEM images and Fourier transform results from left to right, respectively.

3.4. Final optimization of the spin conditions

After obtaining the optimal NS suspension concentration for each NS size under the same spinning conditions, a further study of the spin conditions was conducted using the optimal concentrations. For 0.2µm NS films, the monolayer coverage rate first increases than decreases as the spin speed is increased but the density of grain boundaries does change significantly. As the NS size increases, the effect of spin speed on the monolayer coverage rate and the density of grain boundaries become more and more noticeable. The uniformity of arrays can be further improved by a minor increase of the spin speed for 0.99µm NS films and a minor decrease of spin speed for 0.5µm NS films. Probably a better balance between the centrifuge force and the evaporation rate is achieved here. However, the change of the spin speed is only ~100-200rpm. It is suggested that the NS particles might become charged due to the long sonication time. The electrostatic forces acting between NS particles increases as the NS become smaller. A diluted NS suspension increases the distance between each NS particle and thus suppresses the charge accumulation effects. However, both voids and non-close-packed regions tend to appear when using an overly dilute NS suspension. Thus, for small size PSNS, it is more challenging to obtain an optimal concentration and spinning conditions and form large-area defect-free monolayers. A careful balance must be struck between enough material to achieve a high coverage rate and sufficient distance for avoiding charge accumulation. Moreover, since the optimal NS suspension concentration trend obtained here is based on a specific spinning recipe, there may existother optimal NS suspension concentrations when using higher spin speeds. Nevertheless, it is most economical to use the least NS material possible to achieve the required films.

4. Applications of the NS arrays in plasmonics for photovoltaics

The optimal parameters for spin coating PSNS have been determined. It was found that for different size PSNS, large-area defect-free monolayers can be achieved by using almost the same spinning conditions as long as there is adjustment to the NS suspension concentration. These uniform monolayer films can be used to rapidly fabricate large area plasmonic nanostructures for enhancing light trapping in thin solar cells.

4.1. NS-embedded metallic grating structure

A rear side plasmonic grating structure consisting of metallized (embedded) NS has been numerically studied in detail by Claire E. R. Disney et al [12]. This structure may improve absorption in thin c-Si solar cells and it is proposed that the fabrication of such structures can be easily applied at the final stages of device processing. Figure 8 shows the intended structure and a cross-sectional view of the experimental sample from a 210µm-thick c-Si device.

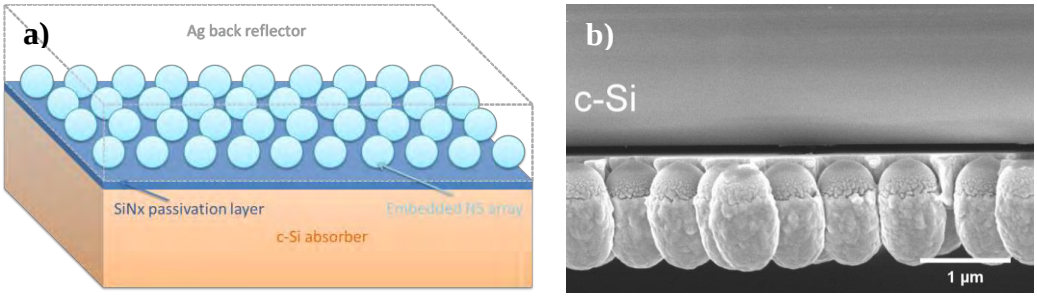

Figure 8 a) Designed and b) SEM cross section images of experimental structure

4.2. Metallic nanodisc array

Periodic metallic nanodisc arrays have also been investigated both numerically and experientially via EBL fabricated optical devices [13][14] Although most studies focus on arrays with square symmetry, Alastair D. Humphrey et. al reported that in determining the optical enhancement due to diffraction, the period of the array is more important than its symmetry [15]. It is therefore useful to apply uniform NS layers as a physical mask to fabricate such structures in large scale devices. Figure 9 shows the intended structure and SEM images of the experimental sample from a 210µm-thick c-Si device. Unfortunately, the uniformity of the array was partially destroyed during the Ar sputter process due to thermal heating. This problem is expected to be resolved by bonding the experimental sample to a heat sink using thermal grease and/or running the sputter process in short cycles.

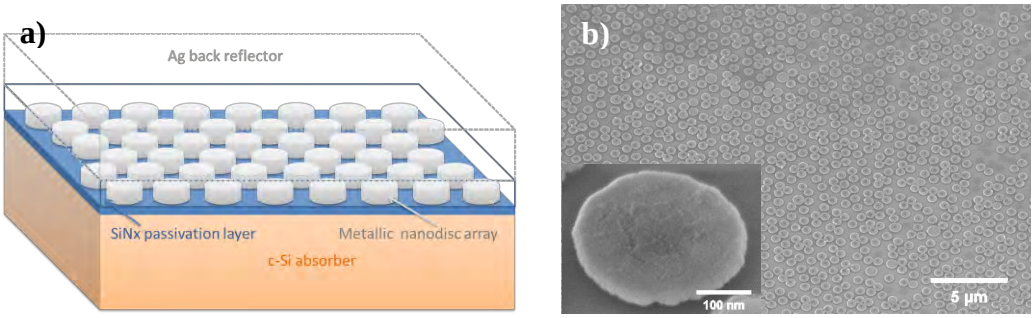

Figure 9 a) Designed and b) SEM images of experimental structure

4.3. Optical device characterization

Both optical devices yield clear absorption enhancement at wavelengths beyond 1000nm, except the metallic nanodisc structure using 0.2μm NS mask films. It is expected that the Ar sputter treatment reduces the radius of the NS by ~100nm, which completely etches the initial 0.2μm NS films, leaving a textured SiNx surface at the rear. Moreover, due to the bonding glue was dissolved during the NS lift-off process, the absorption of the bonding material was not included in the fabricated metallic nanodisc structures. It yields a consistent absorption difference between the planar structure and the fabricated devices. Nevertheless, the absorbance trends shown for both types of samples successfully demonstrate the utility of these uniform NS monolayers for fast and economical fabrication of large scale plasmonic nanostructures.

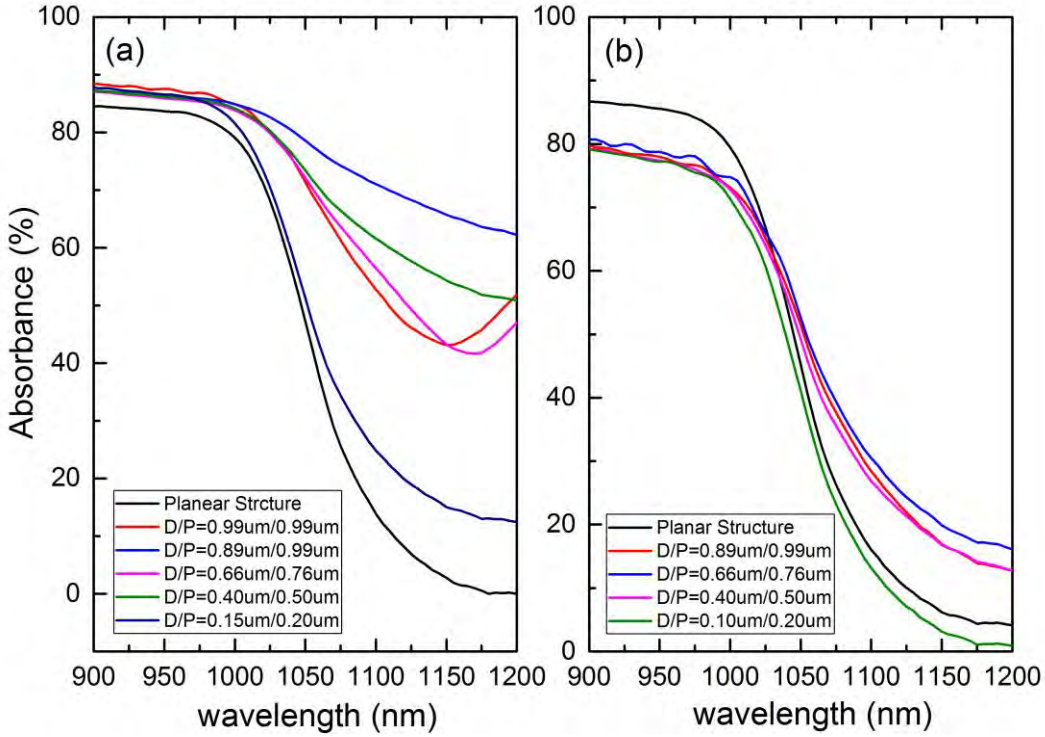

Figure 10 Measured absorbance of a) NS-embedded metallic grating structure and b) metallic nanodisc array structure. The diameter of NS/nanodisc and the pitch of the array are defined as D and P respectively.

5. Conclusions

In this article, the parameters for depositing large-area defect-free monolayers of different size PSNS via spin-coating have been systemically studied. The results show that, for different size PSNS, the concentration of the PSNS suspension has a greater influence than the spin speed and acceleration. By properly adjusting the concentration of the PSNS suspension alone, large scale NS monolayer films can be achieved under almost identical spinning conditions. The optimal concentration of the NS suspensions is noted to be approximately linearly proportional to the size of PSNS. This phenomenon might originate from charge accumulation effects during the sonication treatment required for dispersing the PSNS in suspension. The smaller the NS size, the longer the distance required to minimize the

interparticle Coulombic forces. As a clear demonstration of their utility, two types of large scale plasmonic nanostructures were successfully fabricated via these uniform NS monolayer films. This work can provide guidance for the efficient and controllable deposition of monolayer colloidal films, thereby allowing for the cost-effective fabrication of large scale plasmonic nanostructures for solar cell applications.

References

[1] S. A. Maier, 'Plasmonics: Fundamentals and Applications', *Springer Berlin Heidelberg.*

[2] A. Adibi, T. W. Hänsch, F. Krausz, B. A. J. Monemar, H. Venghaus, H. Weber, and H. Weinfurter, 'Plasmonics From Basics to Advanced Topics', *Springer Berlin Heidelberg.*

[3] H. a Atwater and A. Polman, 'Plasmonics for improved photovoltaic devices', *Nat. Mater.*, vol. 9, no. 3, pp. 205–13, Mar. 2010.

[4] P. Colson, C. Henrist, and R. Cloots, 'Nanosphere Lithography: A Powerful Method for the Controlled Manufacturing of Nanomaterials', *J. Nanomater.*, vol. 2013, pp. 1–19, 2013.

[5] H. W. Deckman and J. H. Dunsmuir, 'Natural lithography', *Appl. Phys. Lett,* vol. 377, no. 1982, pp. 2–5, 2016.

[6] J. C. Hulteen, 'Nanosphere lithography: A materials general fabrication process for periodic particle array surfaces', *J. Vac. Sci. Technol. A Vacuum, Surfaces, Film.*, vol. 13, no. 3, p. 1553, May 1995.

[7] P. Colson, R. Cloots, and C. Henrist, 'Experimental Design Applied to Spin Coating of 2D Colloidal Crystal Masks : A Relevant Method ?' ,*Langmuir*, pp. 12800–12806, 2011.

[8] J. Choi, T. L. Alford, and C. B. Honsberg, 'Solvent-Controlled Spin-Coating Method for Large-Scale Area Deposition of Two-Dimensional Silica Nanosphere Assembled Layers', *Langmuir*, vol. 30, no. 20, pp. 5732–5738, May 2014.

[9] J. Chen, P. Dong, D. Di, C. Wang, H. Wang, J. Wang, and X. Wu, 'Controllable fabrication of 2D colloidal-crystal films with polystyrene nanospheres of various diameters by spin-coating', *Appl. Surf. Sci.*, vol. 270, pp. 6–15, Apr. 2013.

[10] S. S. Shinde and S. Park, 'Oriented colloidal-crystal thin films of polystyrene spheres via spin coating', *Journal of Semiconductors*, vol. 36, no. 2, pp. 1–8, 2015.

[11] T. J. Rehg and B. G. Higgins, 'Spin Coating of Colloidal Suspensions', *AIChE Journa,* vol. 38, no. 4, 1992.

[12] C. E. R. Disney, S. Pillai, C. M. Johnson, and M. A. Green, 'Self-Assembled Nanostructured Rear Reflector Designs for Thin-Film Solar Cells', *ACS Photonics*, pp. 1108–1116, 2015.

[13] S. Mokkapati, F. J. Beck, a. Polman, and K. R. Catchpole, 'Designing periodic arrays of metal nanoparticles for light-trapping applications in solar cells', *Appl. Phys. Lett.*, vol. 95, no. 5, p. 053115, 2009.

[14] D. N. R. Payne, 'The characterization and enhancement of light scattering for thin solar cells', *PhD dissertation*, Uni of Southampton, UK. 2014.

[15] A. D. Humphrey and W. L. Barnes, ‘Plasmonic surface lattice resonances on arrays of different lattice symmetry’, *APS Phys.*, vol. 075404, pp. 1–8, 2014.